

Flux-flow instabilities in amorphous Nb_{0.7}Ge_{0.3} microbridgesD. Babić,^{1,*} J. Bentner,² C. Sürgers,³ and C. Strunk²¹*Department of Physics, Faculty of Science, University of Zagreb, Bijenička 32, HR-10000 Zagreb, Croatia*²*Institut für Experimentelle und angewandte Physik, Universität Regensburg, D-93025 Regensburg, Germany*³*Physikalisches Institut, Universität Karlsruhe, D-76128 Karlsruhe, Germany*

(Received 18 July 2003; revised manuscript received 5 January 2004; published 23 March 2004)

We report measurements of the electric field vs current density $[E(J)]$ characteristics in the mixed state of amorphous Nb_{0.7}Ge_{0.3} microbridges. Close to the transition temperature T_c the Larkin-Ovchinnikov theory of nonlinear flux flow and the related instability describes the data quantitatively up to $\sim 70\%$ of the upper critical magnetic field B_{c2} and over a wide electric-field range. At lower temperatures the nonlinearities of $E(J)$ can be described by electron heating which reduces B_{c2} and leads to a second type of flux flow instability, as shown by a scaling analysis of the high-dissipation data.

DOI: 10.1103/PhysRevB.69.092510

PACS number(s): 74.78.Db, 74.40.+k, 74.25.Qt

It was predicted by Larkin and Ovchinnikov (LO) that the $E(J)$ curves of a “dirty” superconductor in the mixed state may exhibit a steep increase long before the depairing current density is reached.¹ This jump—called flux flow instability (FFI)—was originally expected at temperatures T close to T_c and at a critical vortex velocity $u = u_i$ where the quasiparticles inside the driven vortex cores gain enough energy by the electric field to escape into the surrounding superfluid. The runaway occurs because the quasiparticles cannot relax inside the cores during the time a vortex moves for a distance of the coherence length ξ (\sim vortex radius). The vortices shrink and the vortex motion viscosity is reduced, resulting in an increase of the dissipation at the fixed J . The critical velocity is independent of magnetic field B and corresponds to a critical electric field $E_i = u_i B$. Subsequent theory of Bezuglyj and Shklovskij (BS) took into account heating effects due to a finite rate of heat removal to the bath and predicted that pure, nonthermal LO FFI can occur only at $B \leq 0.4B_{c2}$.² Other studies of the LO FFI explored the effects of a spatially nonuniform distribution of the excitations.³ Explanations of the FFI beyond the original or modified LO picture were sought in dynamic vortex lattice crystallization,⁴ depinning phenomena,⁵ appearance of hot spots,⁶ and recently in vortex core expansion due to electron heating at low temperatures.⁷ Irrespective of its microscopic origin, the FFI is characterized by an $E(J)$ region just above E_i where theory predicts $dE/dJ < 0$, i.e., not only a jump but also a hysteresis in $E(J)$, as verified experimentally in Ref. 8. As B is increased the jump disappears and $E(J)$ is turned to a smooth nonhysteretic curve.

Previous analyses of the mechanisms that cause the FFI relied mostly on identification of the jump at $E_i(J_i)$ and discussion of the B and T dependence of E_i , J_i , and other related parameters (u_i , power density $J_i E_i$, etc.). The quantitative description of $E(J)$ extending both below and above E_i has remained an open question. In particular, for the nonhysteretic $E(J)$ one cannot determine E_i by simply recognizing the jump but has to carry out a comparison with theory, which has not been done. Such an investigation in conventional superconductors is lacking possibly due to the usually strong pinning, which complicates treatments of pure flux

flow effects even in simple vortex systems. In high- T_c superconductors the pinning is weak but the form of vortices is in this case less well known, which is complicated further by peculiar fluctuations in the depinned state.⁹ To avoid the mentioned obstacles as much as possible we have chosen a material already proven to be appropriate for studying the fundamental mechanisms of vortex dynamics, namely, amorphous Nb_{0.7}Ge_{0.3} thin film of thickness comparable to ξ .¹⁰ These samples have very weak or negligible pinning over a considerable part of the (B, T) plane and represent a simple classical dirty superconductor with a well-defined vortex structure. We have chosen the microbridge geometry to reduce the measurement current and thus the power dissipation in the sample.

Close to T_c we have found a quantitative agreement with the LO theory up to an unexpectedly high $b = B/B_{c2} \sim 0.7$, in both the close-to-equilibrium flux flow resistivity ρ_f and the $E(J)$ extended over a wide range of J . We show that E_i can be determined even if there is no jump. At lower temperatures the LO description breaks down, which suggests a different origin of the FFI. These data can be explained consistently by electron heating to a temperature T^* above the bath temperature T_0 , which causes a decrease of $B_{c2}(T^*)$ and a transition to the normal state at an electric field $E_c(B)$.

The methods of sample fabrication and determination of superconducting parameters are described in Ref. 10. The measured microbridge, deposited onto an oxidized Si substrate, was 210 μm long, 5 μm wide, 20 nm thick, and had the following parameters of interest: $T_c = 2.75$ K (with a transition width of 0.05 K), the estimated $T = 0$ normal-state resistivity $\rho_n(0) = 3.3 \pm 0.2 \mu\Omega\text{m}$, $-(dB_{c2}/dT)_{T=T_c} \approx 2.6 \text{ T K}^{-1}$, $\xi(0) = 6.8$ nm, and the other Ginzburg-Landau parameters were $\kappa = 103$ and $\lambda(0) = 1.15 \mu\text{m}$. All the sample parameters are within the range of expected values for amorphous Nb_{0.7}Ge_{0.3} thin films. The measurements were performed in a ³He cryostat with rf filtered leads. The dc $E(J)$ characteristics were measured by increasing the applied current at a rate 10 nA s⁻¹ (0.1 MA m⁻² s⁻¹), whereas the magnetoresistivity $[\rho(B, T)]$ measurements were carried out using small currents (1 MA m⁻²) at which

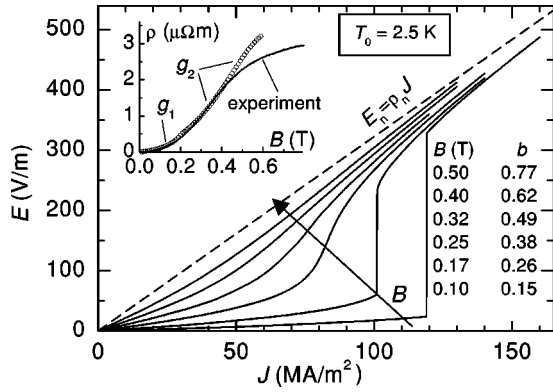


FIG. 1. $E(J)$ at $T_0=2.5$ K, for $0.1 \text{ T} \leq B \leq 0.5 \text{ T}$ ($B_{c2}=0.65 \pm 0.03 \text{ T}$) increasing as indicated by the arrow. The dashed line represents $E_n = \rho_n J$. Inset: Measured magnetoresistivity (solid line) and the LO ρ_f (open symbols) plotted using g_1 and g_2 as explained in the text.

the $E(J)$ is linear, originating from either thermally activated vortex hopping or free flux flow.¹⁰

In Fig. 1 we show $E(J)$ at $T_0=2.5$ K ($t=T_0/T_c=0.91$), for $0.1 \text{ T} \leq B \leq 0.5 \text{ T}$ ($0.15 \leq b \leq 0.77$). A change from an $E(J)$ with the FFI jump (low B) to a smooth $E(J)$ (high B) is clearly visible, as well as a gradual approaching the normal-state electric field $E_n = \rho_n J$ (dashed line) at large J . We show below that the LO FFI theory explains quantitatively all these curves. Close to T_c the LO expression for $J(E)$ is given by

$$J = \sigma_n \left[A + \frac{g(b)}{b(1-t)^{1/2}} Y(E) \right] E, \quad (1)$$

where $\sigma_n = 1/\rho_n$, A is a constant of order unity, $Y(E) = 1/(1+E^2/E_i^2)$ describes the vortex core shrinking, and $g(b)$ is a function approximated by the following interpolation formulas: $g_1(b) = 4.04 - b^{1/4}(3.96 + 2.38b)$ for $b < 0.315$ and $g_2(b) = 0.43(1-b)^{3/2} + 0.69(1-b)^{5/2}$ for $b > 0.315$. In the limit $E \ll E_i$, $Y(E) \approx 1$ and Eq. (1) gives the flux flow resistivity $\rho_f = E/J$. In the expression for ρ_f , $A = 1$ follows from the condition $\rho_f(B_{c2}) = \rho_n$, whereas in nonequilibrium the constant value of $A \approx 1$ reflects suppression of the superconducting order parameter outside the cores by a strong electric field.⁸

A comparison of two typical experimental $E(J)$ characteristics (solid lines) at $T_0=2.5$ K, with ($B=0.1$ T) and without ($B=0.4$ T) the jump, and Eq. (1) (dashed lines) is shown in Fig. 2. Equation (1) agrees with the data excellently by taking $\sigma_n = 3.1 \times 10^5 \text{ S/m}$ from $\rho(B \sim 2B_{c2})$, A ranging from 0.92 to 0.97 with no systematic B dependence, and using $B_{c2} = 0.65 \pm 0.03 \text{ T}$ to calculate $g(b)/b$ and the corresponding error bars [important at low b where $g(b)/b$ is a steep function]. Thus, the only free parameter is E_i , shown in the inset to Fig. 2(a) and discussed later.

In the inset to Fig. 1 we show $\rho(B)$ (solid line) at the same temperature, compared with the theoretical ρ_f (open symbols). With the same values of parameters B_{c2} , σ_n , and A as above, the agreement of the data and the LO theory is

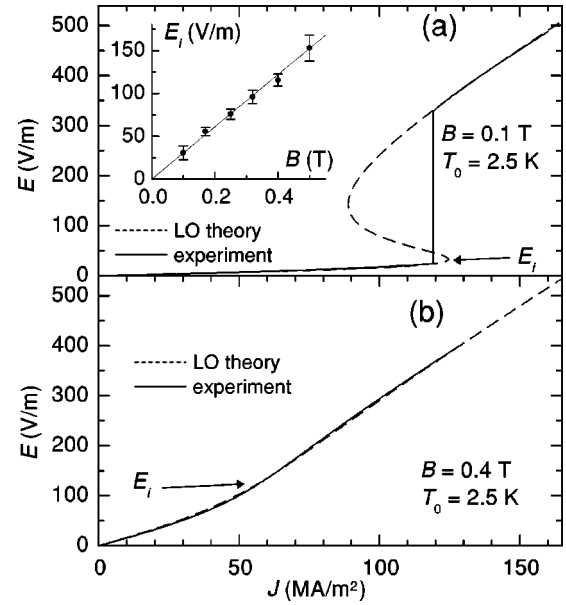


FIG. 2. $E(J)$ at $T_0=2.5$ K (full lines), for (a) $B=0.1$ T and (b) $B=0.4$ T. The dashed lines are plots of Eq. (1) with the appropriate choices of the parameters, as discussed in the text. Inset to (a): Extracted $E_i(B)$ (circles), illustrating the validity of the LO theory with $u_i = E_i/B$ independent of magnetic field.

satisfactory below ~ 0.5 T all the way down to $B \rightarrow 0$. This implies a negligible critical current density J_c and a good description of the close-to-equilibrium transport properties in terms of the LO theory for all the $E(J)$ shown in Fig. 1. The LO theory, however, fails to explain the data closer to B_{c2} , in contrast to our previous finding¹⁰ for another sample at $t=0.82$ and the present sample at $t=0.7$ (not shown). The failure of the LO theory to describe $\rho(B \rightarrow B_{c2})$ in the vicinity of T_c may be related to a widening of the equilibrium critical-fluctuation region at B sufficiently close to B_{c2} .

From the slope of linear $E_i(B)$ we calculate the vortex critical velocity $u_i = 305 \text{ m/s}$. Using the LO expression $u_i = \sqrt{D[14\zeta(3)(1-T/T_c)]^{1/2}/\pi\tau_{e,ph}}$ we can determine the electron-phonon inelastic scattering time $\tau_{e,ph} = 0.18 \text{ ns}$, where $D = 8k_B T_c \xi^2(0)/\pi\hbar = 4.3 \times 10^{-5} \text{ m}^2/\text{s}$ is the diffusion constant and ζ the Riemann zeta function. The corresponding inelastic relaxation length is calculated as $l_{e,ph} = \sqrt{D\tau_{e,ph}} = 87 \text{ nm}$. The linearity of $E_i(B)$ provides strong evidence for the FFI being caused by the LO mechanism of vortex core shrinking. Note that the LO model holds up to an unexpectedly high b , almost twice larger than the upper limit estimated by BS. Only for $B=0.5$ T the relatively large error bar of the corresponding E_i may imply that the BS heating is starting to take place, but the agreement with Eq. (1) is still very good over the whole E range. Previously we showed that the weak heating effects in this regime contributed mostly to the vortex motion noise.¹⁰ In conclusion to this part, our results for T_0 close to T_c are over a large B interval in remarkable quantitative agreement with the LO theory.

We now turn to the low-temperature regime. Recently Kunchur analyzed the FFI in $\text{YBa}_2\text{Cu}_3\text{O}_{7-\delta}$ at low temperatures and small to moderate b in terms of electron heating to a temperature $T^* > T_0$.⁷ Well below T_c the LO mechanism is

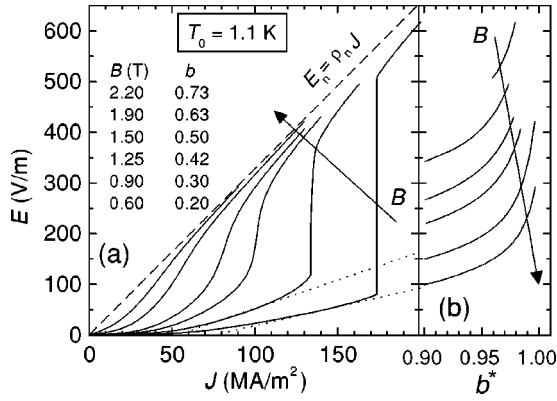


FIG. 3. (a) $E(J)$ at $T_0 = 1.1$ K (solid lines), for $0.6 \text{ T} \leq B \leq 2.2 \text{ T}$ ($B_{c2} = 3.0 \pm 0.1 \text{ T}$) increasing as indicated by the arrow. The dashed line shows $E_n = \rho_n J$. The dotted lines are plots of $J = 0.9\sigma_n / (b + J_c)$ for 0.6 T and 0.9 T . (b) E vs b^* calculated from the measured $E(J)$ and Eq. (2) using $\alpha = 3$. The vertical scale is the same as in (a) and the arrow points again in the direction of increasing B .

expected to be ineffective since in this case the superconducting order parameter does not depend strongly on small changes of the electron distribution function.¹ On the other hand, at low T the efficiency of heat removal from electrons to phonons, as well as from phonons to the bath, is reduced and a nonequilibrium suppression of superconductivity by electron heating appears natural. This effect can be conveniently expressed through a decrease of $B_{c2}(T^*)$. In order to investigate the differences and/or similarities between the FFI and overall nonlinearities of the $E(J)$ at low and high T we carried out measurements at $T_0 = 1.1 \text{ K}$ ($t = 0.4$) over a similar range of b as before, the results of which are shown in Fig. 3(a). Despite the apparent similarity of the curves when compared to those of Fig. 2, we did not obtain any satisfactory agreement with Eq. (1) even if we left all the numerical parameters floating and/or replaced the b -dependent part with the ones appropriate at low temperatures (see below). This motivated us to analyze these results in terms of electron heating as the cause of a second type of the FFI.

At low t and b the equilibrium dissipation is described by $J(E) = J_c + 0.9\sigma_n E / b$.¹ The plots of this expression are shown by the dotted lines in Fig. 3(a) for 0.6 T and 0.9 T . We used $B_{c2} = 3.0 \pm 0.1 \text{ T}$ as determined from $\rho_f(B)$, thus J_c was the only free parameter. The replacement $T_0 \rightarrow T^*$ can explain the rise of $E(J)$ above the dotted lines by a progressive decrease of J_c and increase of b (by the suppression of B_{c2}). The decrease of $B_{c2}(E)$ implies a nonmonotonic dependence of the ratio $E/b(E)$ on E , resulting in a negative slope of $J(E)$, and causing a flux flow instability of the origin different than the LO core shrinking. This regime of low to moderate b was analyzed in detail by Kunchur, but due to the large B_{c2} in high- T_c compounds the limit $B \rightarrow B_{c2}$ (i.e., $E \rightarrow E_n$) remained unexplored. In our experiment B_{c2} is accessible, which permits a complementary test of the electron-heating approach, as presented below.

In order to analyze the $E(J) \rightarrow E_n$ data we recall another LO result, namely, that as long as the electron mean free path

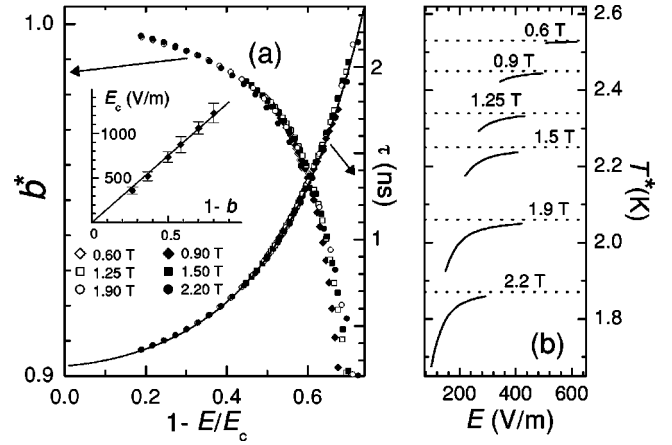


FIG. 4. (a) Scaling plot of the nonequilibrium reduced magnetic field b^* (left-hand scale) and the quasiparticle scattering time τ (right-hand scale) vs $1 - E/E_c$, as indicated by the arrows and calculated as explained in the text. The solid line represents $\tau = \tau_0 \exp[3.5(1 - E/E_c)^{3/2}]$ with $\tau_0 \approx 0.25 \text{ ns}$. Inset: E_c against equilibrium $1 - b$. The error bars indicate how much E_c varies if the scaling of b^* is performed using α between 2 and 4. (b) The electron temperature T^* (solid lines) vs E for different B , estimated from the equilibrium $B_{c2}(T)$ characteristics. The dotted lines represent $T_c(B)$.

is much smaller than ξ , close to B_{c2} the $J(E)$ is at an arbitrary temperature determined by¹

$$J = \sigma_n [1 + \alpha(T)(1 - b)]E, \quad (2)$$

where α is a temperature-dependent constant varying between 2 and 4, and J_c at such high dissipation can be disregarded. If the assumption of electron-heating-induced nonlinearities is correct, Eq. (2) should describe the upper part of $E(J)$ through E dependence of b and α up to the transition to the normal state at a critical electric field $E_c(B)$ corresponding to $T^* = T_c(B)$ [equivalently, to $B = B_{c2}(T^*)$]. In other words, b increases to a nonequilibrium $b^*(E)$. If the temperature dependence (and hence the E dependence) of α is weak,¹ we can approximate α by a constant and invert Eq. (2) to calculate $b^*(E) = B/B_{c2}(E)$ from our $E(J)$ data. In Fig. 3(b) we show a plot of E vs b^* (calculated using $\alpha = 3$) for $b^* > 0.9$, where we expect the validity of Eq. (2) and the approximation of a constant α . The similarity of these curves for different values of B suggests a possible scaling $b^*(E/E_c)$ for a proper choice of $E_c(B)$. This is demonstrated in Fig. 4(a), where $E_c(B)$ is chosen such that b^* (left-hand scale) scales with $1 - E/E_c$, i.e., the data shown in Fig. 3(b) can be collapsed onto the same curve. Using the obtained values of $B_{c2}(E) = B/b^*(E)$ and the equilibrium $B_{c2}(T)$ characteristics we can estimate the values of $T^*(E)$ for each B , as shown in Fig. 4(b) by the solid lines. As the heating progresses, T^* approaches $T_c(B)$ (horizontal dotted lines).

The above procedure corresponds to a determination of $E_c(B)$, shown in the inset to Fig. 4(a) by symbols. The solid line represents $E_c = E_{c0}(1 - b)$, and describes the inferred values of E_c fairly well in terms of a phenomenological parameter $E_{c0} = 1500 \text{ V/m}$. This result can be made plausible if

we analyze our results further with regard to the thermodynamic properties of the mixed state. The electron-heating model¹¹ assumes that the stationary state at T^* is established according to $JE\tau = G_s(T_0) - G_s(T^*)$, where G_s is the superconducting part of the Gibbs free-energy density and τ the relaxation time of the nonequilibrium state.¹² At $E = E_c$ the above equation leads to $\sigma_n E_c^2 \tau_0 = G_s(T_0)$, τ_0 being the relaxation time at the $E_c(B)$ phase boundary, where the superconductivity is destroyed. Since for a dirty high- κ superconductor at large b we can take $G_s = U_s(1-b)^2$, where $U_s = B_{c2}^2/4\mu_0\kappa^2$ is the zero- B superconducting condensation energy,¹³ we obtain $E_c \propto 1-b$, which agrees with our scaling result and links τ_0 with E_{c0} .

Having found an explanation for the linearity of E_c vs $1-b$ we can proceed to calculate $\tau = [G_s(T_0) - G_s(T^*)]/JE$ by inserting the values of $B_{c2}(E)$ [see Fig. 4(a)] into the expression for $G_s(T^*) = G_s(E)$. Again, we obtain a scaling behavior of τ with respect to $1 - E/E_c$, as we show in Fig. 4(b) by symbols (right-hand scale). Note that this scaling is not a simple consequence of the scaling of b^* extracted from Fig. 3(b), since $B_{c2}^2(E)$ enters the expression for $U_s(E)$ independently. The obtained result can be described phenomenologically by $\tau(E, B) = \tau_0 \exp\{3.5[1 - E/E_c(B)]^{3/2}\}$, with $\tau_0 \approx 0.25$ ns. This is illustrated by the solid line in Fig. 4(a). The relaxation of the nonequilibrium state most likely occurs through the recombination of quasiparticles accompanied with the emission of nonequilibrium phonons, typical of the response of a superconducting film to energy deposition.¹⁴ The scattering rate in this process depends on the quasipar-

ticle density, which is controlled by the energy gap and temperature. Although the above expression for $\tau(E, B)$ is descriptive only, we note that the $(1 - E/E_c)^{3/2}$ exponential dependence could possibly be related to a suppression of the gap by approaching the nonequilibrium phase boundary $E_c(B)$. This issue requires further investigation, together with our finding that critical fluctuations around B_{c2} seem to affect ρ_f in complete thermal equilibrium close to T_c but not $E(J)$ at $T_0 \ll T_c$ even if $B \rightarrow B_{c2}$ by electron heating.

In conclusion, we have measured and analyzed the $E(J)$ curves of amorphous $\text{Nb}_{0.7}\text{Ge}_{0.3}$ microbridges over a wide range of magnetic field and in two characteristic regimes, i.e., close to and well below T_c . In the former case we have found an excellent agreement with the Larkin-Ovchinnikov theory of nonlinear flux flow and the related instability up to $B/B_{c2} \sim 0.7$, which is much larger than predicted theoretically by Bezuglyj and Shklovskij. At low temperatures the nonlinearity of $E(J)$ and the flux flow instability can be reasonably well described by electron heating and the related decrease of B_{c2} . The corresponding striking scaling of $E(J)$ and $\tau(E, B)$ calls for a more detailed theoretical analysis in order to understand the underlying microscopic mechanisms.

We thank F. Rohlfing, W. Meindl, B. Stojetz, A. Bauer, and M. Furthmeier for technical support. This work was partially funded by the Deutsche Forschungsgemeinschaft within the Graduiertenkolleg 638. Additional support by the Croatian Ministry of Science (Project No. 119262) and the Bavarian Ministry for Science, Research and Art is gratefully acknowledged.

*Corresponding author. Electronic address: dbabic@phy.hr

¹A. I. Larkin and Yu. N. Ovchinnikov, in *Nonequilibrium Superconductivity*, edited by D. N. Langenberg and A. I. Larkin (North-Holland, Amsterdam, 1986).

²A.I. Bezuglyj and V.A. Shklovskij, *Physica C* **202**, 234 (1992).

³S.G. Döttinger, R.P. Hübener, and A. Kühle, *Physica C* **251**, 251 (1995).

⁴A.E. Koshelev and V.M. Vinokur, *Phys. Rev. Lett.* **73**, 3580 (1994).

⁵J.A. Fendrich *et al.*, *Phys. Rev. Lett.* **77**, 2073 (1996); W. Henderson *et al.*, *ibid.* **77**, 2077 (1996).

⁶Z.L. Xiao, E.Y. Andrei, and P. Ziemann, *Phys. Rev. B* **58**, 11 185 (1998).

⁷M.N. Kunchur, *Phys. Rev. Lett.* **89**, 137005 (2002).

⁸A.V. Samoilov *et al.*, *Phys. Rev. Lett.* **75**, 4118 (1995).

⁹D. Babić *et al.*, *Phys. Rev. B* **60**, 698 (1999).

¹⁰D. Babić *et al.*, *Phys. Rev. B* **66**, 014537 (2002).

¹¹M. Kankar, M.N. Wybourne, and K. Johnson, *Phys. Rev. B* **47**, 13 769 (1993).

¹²Here we have disregarded the change of the normal part of Gibbs energy by the heating, which seems to be an acceptable approximation. Otherwise the linear E_c vs $1-b$ plot would have a noticeable intercept at $1-b=0$.

¹³A. L. Fetter and P. C. Hohenberg, in *Superconductivity*, edited by R. D. Parks (Marcel Dekker, New York, 1969).

¹⁴A. Rothwarf and B.N. Taylor, *Phys. Rev. Lett.* **19**, 27 (1967).